WAVE NORMAL DIRECTION OF AURORAL HISS OBSERVED BY THE S-310JA-5 ROCKET

Iwane KIMURA and Toshio MATSUO

Department of Electrical Engineering II, Kyoto University, Yoshida-Honmachi, Sakyo-ku Kyoto 606

Abstract: Wave normal directions of auroral hiss observed by the S-310JA-5 rocket are analyzed from the spin modulation data of electric field components picked up by a dipole antenna extended perpendicular to the rocket axis, and the angle between the wave normal direction and the rocket axis observed by the crossed loop antennas which are both perpendicular to the rocket axis. It is found that the wave normals were making large angles to the magnetic meridian plane, so that the ray paths tracing back to the source indicate an altitude which is not above 700 km, when the electron and ion temperature are less than 800 K. The electron density between 200 km and 230 km actually observed by same rocket showed a density gradient much less than that represented by the plasma temperature of 800 K. This point will support our result for the source altitude of auroral hiss observed by rocket.

1. Introduction

Measurements of wave normal and Poynting vector directions of auroral hiss emissions were made by using an Antarctic rocket S-310JA-5, which was launched at Syowa Station at 2256:50 UT on 10 June 1978.

This experiment was successful and it was found that the Poynting energy flow was downward and the angle between the wave normal and the rocket axis was approximately 70° to 80°. We also tried to measure the direction of Poynting vector from the pitch angle dependency of the rocket axial component of the Poynting flux density, P_z, which was calculated from the components of electric (E) and magnetic (H) fields perpendicular to the rocket axis (in detail, refer to KIMURA *et al.*, 1981, which hereafter is called paper I). If this measurement had been successful, we could have determined the absolute direction of the wave normal using this determination of Poynting flux.

Actually a DC component of P_z was obtained and it was found that the energy flow was downward. However the AC component of rocket spin frequency, which is necessary to calculate the absolute direction of Poynting flux could not be determined.

The wave normal direction with reference to the rocket axis was calculated by using the magnetic field components perpendicular to the rocket axis, which were measured by crossed air-core antennas.

In this experiment the dynamic spectrum showed a clear intensity variation due to the rocket spin motion. Such an intensity modulation is considered to have, in addition, information on the wave normal direction. In the present paper, we will

185

report the result of analysis of the wave normal direction derived from the rocket spin modulation of the signal intensity.

2. Method of Analysis

If the observed auroral hiss was propagating in the whistler mode and if the direction of the wave normal and the signal intensity are assumed to be known and constant with time, the intensity variation due to the rocket spin motion can be calculated. If we can find a wave normal direction which produces a spin modulation best fitting the observed one, that direction will be the one which we wish to know.

As was previously mentioned, we have measured the angle between the wave normal angle and the rocket spin axis, so that we can eliminate one freedom in the assumption of the wave normal direction.

Calculation of intensity modulation due to the rocket spin motion

First, we describe how to calculate the intensity modulation of signals observed by the dipole antenna which was extended perpendicularly to the rocket axis, based upon the assumptions that the wave normal direction is known and that it does not change over the spin period which is about 1 s in our experiment.

At first, rectangular coordinates x, y, z are taken so that the z-axis lies in the direction of the geomagnetic field and the wave normal vector k is in the x–z plane making an angle θ with z as shown in Fig. 1. In this coordinate system, the polarization of electric field components is as follows:

$$\left. \begin{aligned} E_z &= -\frac{n^2 \sin\theta \cos\theta}{P - n^2 \sin^2\theta} E_x \\[2mm] E_y &= \frac{jD}{S - n^2} E_x \end{aligned} \right\} \tag{1}$$

and the x, y, z components of the wave magnetic field are

$$\left. \begin{aligned} H_x &= -\frac{nE_y}{Z_0} \cos\theta \\[2mm] H_y &= \frac{n}{Z_0}(E_x \cos\theta - E_z \sin\theta) \\[2mm] H_z &= \frac{n}{Z_0} E_y \sin\theta \end{aligned} \right\} \tag{2}$$

where n and Z_0 are the refractive index and space impedance in vacuum ($120\,\pi\Omega$), and S, D, and P are the quantities defined by STIX (1962), in which the effects of ions can be taken into account. The effect of collisions will be neglected in the following analysis.

In this coordinate system, the time average Poynting flux S_p has only x and z components and the magnitude of the averaged flux is

$$\bar{S}_p = \frac{n}{2Z_0} |E_x|^2 \left[\left\{ \left(\frac{D}{S-n^2}\right)^2 + \frac{Pn^2 \cos^2\theta}{(P - n^2 \sin^2\theta)^2} \right\}^2 \sin^2\theta \right.$$
$$\left. + \left\{ \frac{P}{P - n^2 \sin^2\theta} + \left(\frac{D}{S - n^2}\right)^2 \right\}^2 \cos^2\theta \right]^{1/2} . \tag{3}$$

Fig. 1. The initial coordinate system, *x*, *y* and
z for the wave normal direction $\vec{k}$ and
the geomagnetic field B_0, and the rota-
tionally transformed coordinate sys-
tems, *x'*, *y'* and *z'*, and *x''*, *y''* and *z''*,
where *z''* is directed along the rocket
spin axis ($\vec{R}$).
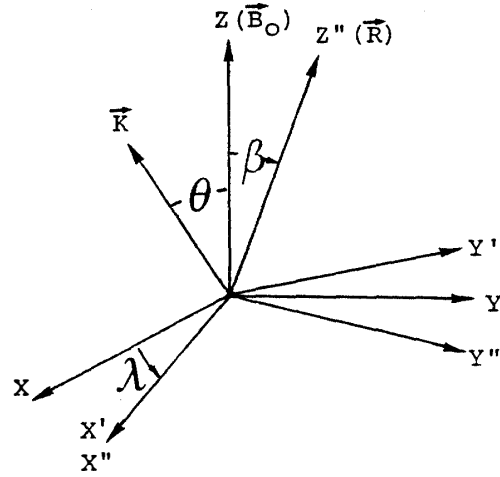
In order to calculate the signal intensity in the plane perpendicular to the rocket axis, we transform the coordinate system to one related to the rocket attitude. For this transformation, as shown in Fig. 1, we first rotate the *x*, *y*, *z* system by an angle λ around the *z* axis to get a new system $x', y', z'(z)$. Then we rotate the x', y', z' system by an angle β around the *x'* axis to get the final system $x''(x'), y'', z''$.

By such two rotational transformations, we can make the direction of *z''* to coincide with the rocket axial direction ($\vec{R}$). By these transformations, the electric field components, E_x'' and E_y'', perpendicular to the rocket axis are represented by

$$\left. \begin{array}{l} E_x'' = E_x \cos \lambda + E_y \sin \lambda \\ E_y'' = -E_x \cos \beta \sin \lambda + E_y \cos \beta \cos \lambda - E_z \sin \beta \end{array} \right\} . \qquad (4)$$

Actually, we know the angle β experimentally from the data of a geomagnetic aspect-meter on board the rocket. The angle (ϕ) between the *k* vector and the rocket axis (z'') can be obtained also from the experiment, so that if we arbitrarily assign λ, we can determine principally two values of θ by spherical trigonometry by the following relation,

$$\cos \theta = \frac{\cos \phi \cos \beta \pm \sqrt{\cos^2 \phi \cos^2 \beta - (\cos^2 \beta + \sin^2 \beta \sin^2 \lambda)(\cos^2 \phi - \sin^2 \beta \sin^2 \lambda)}}{\cos^2 \beta + \sin^2 \beta \sin^2 \lambda} . \qquad (5)$$

In this equation, the $\pm$ sign in front of the square root must be opposite for $\lambda = 0°$ to 180° and for $\lambda = 180°$ to 360° for the sake of continuity of θ with λ.

From our experiment, we have determined that the Poynting flux was downward so that θ must be larger than 90°. Therefore we can select the proper one for θ from the two solutions of eq. (5). Once θ is known for an assumed λ, we can calculate *n*, *S*, *D* and *P* for actually observed plasma parameters and the polarization relations in the *x*, *y*, *z* coordinate system are determined, then E_x'' and E_y'' by eq. (4).

The output of a dipole antenna on board the rocket, depending on the rocket spin motion is represented by

$$|V| = |E_x'' \cos \Omega_s t + E_y'' \sin \Omega_s t|$$
$$= [\{R_e(E_x'') \cos \Omega_s t + R_e(E_y'') \sin \Omega_s t\}^2 + \{I_m(E_x'') \cos \Omega_s t + I_m(E_y'') \sin \Omega_s t\}^2]^{1/2} , \qquad (6)$$

where Ω_s is the angular frequency of the rocket spin and t is zero when the antenna line is directed along the x'' axis. $R_e(\ )$ and $I_m(\ )$ are the real and imaginary parts of the bracketed quantity. Using eqs. (1) and (4), we have

$$\left.\begin{aligned}
R_e(E_x'') &= |E_x|\cos\lambda \\
I_m(E_x'') &= \frac{D}{S-n^2}|E_x|\sin\lambda \\
R_e(E_y'') &= \left\{\frac{n^2\sin\theta\cos\theta}{P-n^2\sin^2\theta}\sin\beta-\cos\beta\sin\lambda\right\}|E_x| \\
I_m(E_y'') &= \frac{D}{S-n^2}|E_x|\cos\beta\cos\lambda
\end{aligned}\right\}. \qquad (7)$$

For each λ, we can calculate the angle θ as mentioned previously. Then we have to know the angle η between k and the vertical and then the angle ξ or azimuthal angle of k vector from the geomagnetic north. These angles are calculated using spherical trigonometry as follows:

$$\left.\begin{aligned}
\eta &= \cos^{-1}\{\cos\theta\cos\psi-\sin\theta\sin\psi\sin(\lambda-\gamma)\} \\
\xi &= \sin^{-1}\left\{\frac{\sin\theta}{\sin\eta}\cos(\lambda-\gamma)\right\}
\end{aligned}\right\}, \qquad (8)$$

where ψ is the angle between $\vec{B}_0$ and the vertical, and γ is the angle between the $\vec{R}-\vec{B}_0$ plane and the geomagnetic meridian plane, which is calculated by using the zenith angle ρ of the rocket attitude, the angle β between $\vec{B}_0$ and $\vec{R}$, and ψ. γ is assigned positive when the rocket axis is directed to the east of the geomagnetic meridian plane and ξ is positive for the counter clockwise direction from the geomagnetic north. 180-ξ is also another possible value of ξ. Therefore we have to select the proper one so that ξ varies continuously with the variation of λ from 0 to 360°.

With these ξ and η, we can determine ε and δ, which are the angle between the k vector and the geomagnetic meridian plane and the angle between the vertical (radial) direction and the projection of k onto the geomagnetic meridian plane, respectively, as follows:

$$\left.\begin{aligned}
\sin\varepsilon &= \sin\xi\sin\eta \\
\tan\delta &= \tan\eta\cos\xi
\end{aligned}\right\}, \qquad (9)$$

ε is taken positive when the k vector lies to the west of the meridian plane from eq. (9), and δ is positive when the k vector leans toward north from the vertical. ε and δ have some ambiguity. Therefore the proper ones must be chosen so that the wave normal angle θ, which can be determined by the direction cosines of the k vector and geomagnetic field direction, is the same as the θ used to determine ξ and η. The ε and δ thus obtained will be used for 3-dimentional ray tracing.

Finally, we can draw the spin modulation patterns for the angle ξ from 0 to 360°, instead of for the angle λ. A necessity for ξ is that the observed spin modulation pattern is drawn in a polar graph as a function of this angle.

3. Experimental Data

An example of the observed hiss spectra is shown in Fig. 2. From this spectrum, it is evident that the instances showing maximum and minimum in signal intensity are simultaneous for frequencies between 4.5 and 7 kHz. This fact implies that the all frequency components in this range reached the rocket from the same direction. This is not always the case, because at an altitude around 223 km, the hiss spectra
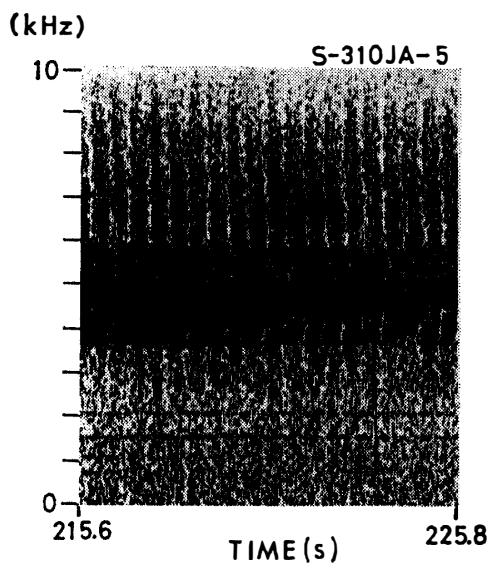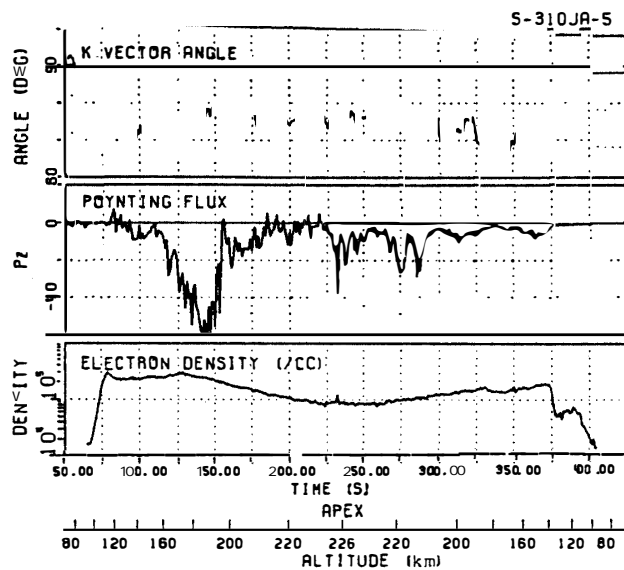

Fig. 2. *A sample of the dynamic spectrum of auroral hiss.*

Fig. 3. *Variation of the wave normal direction, Poynting flux and electron density versus time after launch and altituce.*
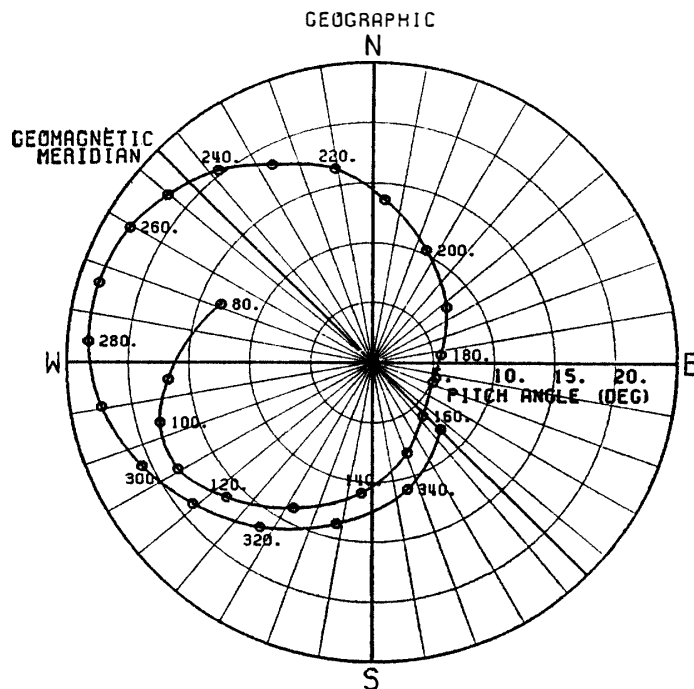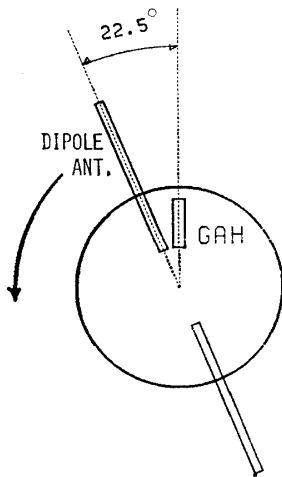

Fig. 4. *Time variation of the rocket attitude.*

Fig. 5. Configuration of
         the dipole an-
         tenna and geo-
         magnetic aspect
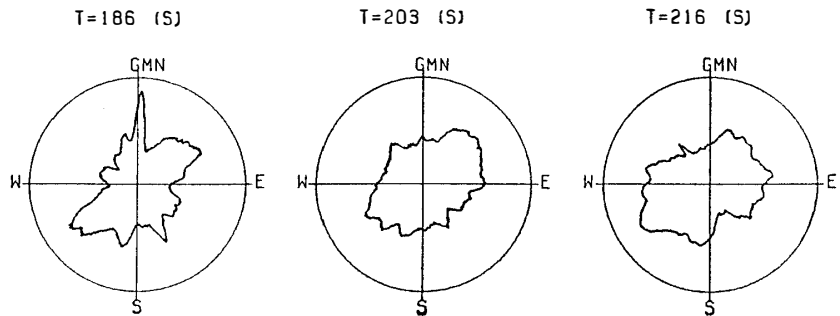   sensor (GAH).

Fig. 6. Examples of spin modulation patterns of the hiss intensity.

have shown a dispersion, the maximum and minimum delayed in time for the lower frequencies, as shown in Fig. 10 of paper I.   However, in the following analysis we will use data similar to that shown in Fig. 2.

The wave normal angle relative to the rocket axis, measured at 7 kHz by crossed loop antennas on board the rocket is illustrated in Fig. 3, together with other quantities observed by the same rocket, i.e. Poynting flux at 7 kHz and electron density.   In these results, the observed wave normal angle ϕ referring to the rocket axis has an ambiguity between ϕ and 180-ϕ.   Therefore we have to consider both cases for the following analysis.

The direction of the rocket axis during flight is plotted in Fig. 4 in a polar diagram with the zenith at the center.   Each point on the plot corresponds to the zenith angle and the azimuthal angle of the rocket at the time(s) after launch, as indicated in the diagram.   Figure 5 shows the direction of the dipole antenna, whose output will be used for analysis, relative to the direction of geomagnetic aspect sensor (GAH) as viewed from the top of the rocket.   The arrow in the figure indicates the direction of spin rotation of the rocket.

Taking account of a delay time in the telemetry channel for GAH, the dipole antenna output leads the GAH output by 30.9° in spin phase.   From the phase of the signal at the instant when the output of GAH becomes maximum, the directional characteristics of the spin modulation of the signal can be deduced.

As seen in Fig. 2, the signal intensity at 7 kHz, at which time the wave normal angle relative to the rocket axis was measured, was weak compared with those at frequencies lower than 7 kHz.   In the following analysis, the spin variation data at 6.5 kHz will be used, based on the assumption that the 6.5 kHz signal came to the rocket from the same arrival direction as that of the 7 kHz signal.

In Fig. 6 are polar plots of the spin variation at t=186, 203 and 216 s after launch.   The AGC effect of the rocket borne receiver has been compensated.   Such
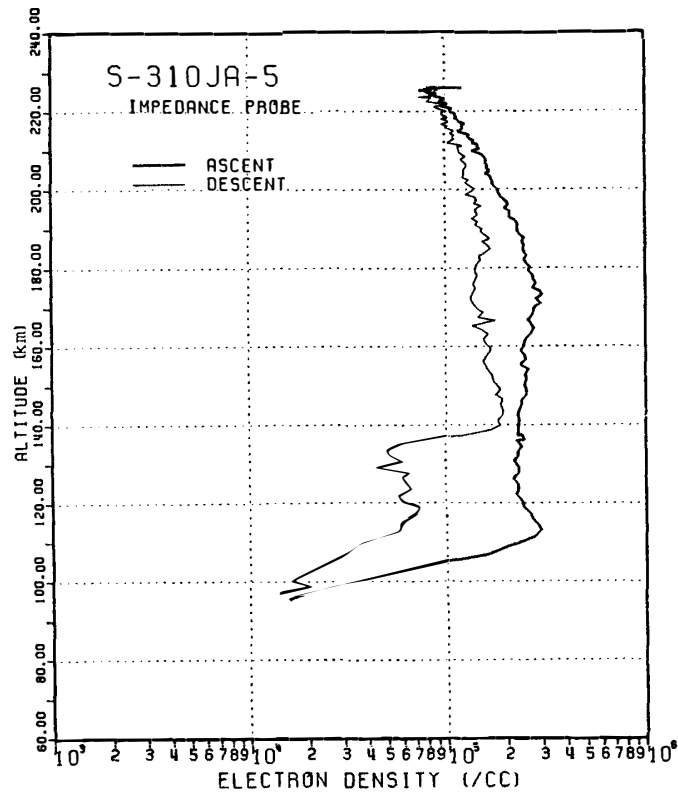
Fig. 7.   Electron density profiles observed by the rocket.

a plot can be drawn for every spin period, approximately 1 s, and does not always show the same pattern in time. This is because the source location and intensity of auroral hiss observed might have changed very quickly. However, around the above times, the shapes of the several spin patterns were relatively similar. Several such instance are selected for the following analysis of the arrival direction of the hiss.

In order to find an appropriate direction of the k vector, we will draw theoretically calculated spin modulation patterns for each direction of ξ. For the calculation, the electron density to be used is based on the profile observed by the same rocket, which is shown in Fig. 7. Ion effects are taken into account by the quantities; $NO^+=45\%$, $O_2^+=45\%$, and $O^+=10\%$. The geomagnetic dip angle used is $65.5°$.

For the case of $t=203$ s, the rocket attitude was such that the zenith angle $\rho=11.5°$, $\gamma=28.7°$ and the angle β between $\vec{B}_0$ and the rocket axis is equal to $21.5°$. The angle ϕ between the rocket axis and the k vector was observed to be $76°$ or $(180°-76°)$. For this ϕ we calculate θ for $\lambda=0$ to $360°$. We have two solutions of θ for a given λ as shown by eq. (5) and have to select a θ which is larger than $90°$, because the Poynting vector observed was directed downward as mentioned previously. Thus, there are four kinds of solutions of θ for two possible values of ϕ as follows:

(A) $\phi=104°$, $+$sign for $\lambda=0°$ to $180°$ and $-$sign for $\lambda=180°$ to $360°$ are taken in eq. (5).

(B) $\phi=104°$, opposite sign in eq. (5) compared with case (A).

(C) $\phi=76°$, $+$sign for $\lambda=0°$ to $180°$ and $-$sign for $\lambda=180°$ to $360°$ in eq. (5).
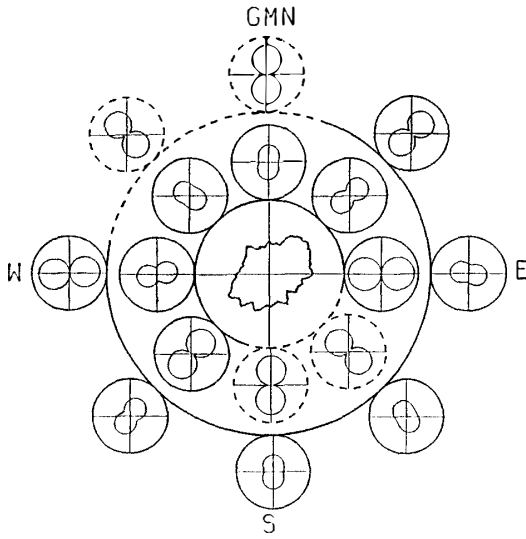
Fig. 8. Calculated spin modulation patterns as
a function of the incoming wave normal
direction along with the observed one in
the center.

(D) $\phi=76°$, opposite sign in eq. (5) compared with case (C). Inserting these
quantities λ, θ, in addition to the known values of γ and ϕ into eq. (8), η and ξ are
calculated.

In Fig. 8 the calculated spin modulation patterns are illustrated for every 45° of
ξ starting from $\xi=0°$ (geomagnetic north (GMN)). Actually we need to draw the
diagram for the incoming direction of the k vector to the rocket. However, the angle ξ
was taken as the direction of the k vector outgoing from the rocket. Therefore in Fig. 8,
each pattern is distributed peripherally, taking account of this fact. These spin modula-
tion patterns for different ξ are produced under the restriction that the Poynting flux
given by eq. (3) is constant for any ξ. In this figure, the above four cases (A) to (D)
are illustrated in such a way that calculated spin modulation patterns arranged inside
the large circle and drawn by solid lines correspond to case (A), those arranged inside
and drawn by dashed lines to case (D), those outside and solid lines to case (B) and
dashed lines to case (C). Fortunately, (A) and (D), and (B) and (C), are complemen-
tary with respect to the coverage of ξ for $\theta > 90°$.

The observed spin modulation pattern is illustrated in the central circle. By
comparing the calculated patterns with observed one, which shows no sharp minimum
at any azimuthal direction, the incident direction seems to be around 45° east from the
geomagnetic north (GMN) ($\xi \simeq 135°$) for case (A) and 135° west from GMN ($\xi \simeq 315°$)
for case (B). It turns out that there are two possible solutions for the wave normal
direction.

For each given ξ, the directions of the wave normal are given for the above four
cases. Then δ and ε can be calculated, where ε is the angle between k vector and the
geomagnetic meridian plane and δ is the angle between the radial direction and the
projection of the k vector onto the geomagnetic meridian plane. Figures 9(A) to
9(D) show δ, ε and θ plotted against ξ for cases (A) to (D).

Corresponding to the two solutions of the wave normal directions, which are
obtained by comparing with the observed data as mentioned above, we have two
pairs of ε and δ, by which we can trace the ray paths backwards up to their source.
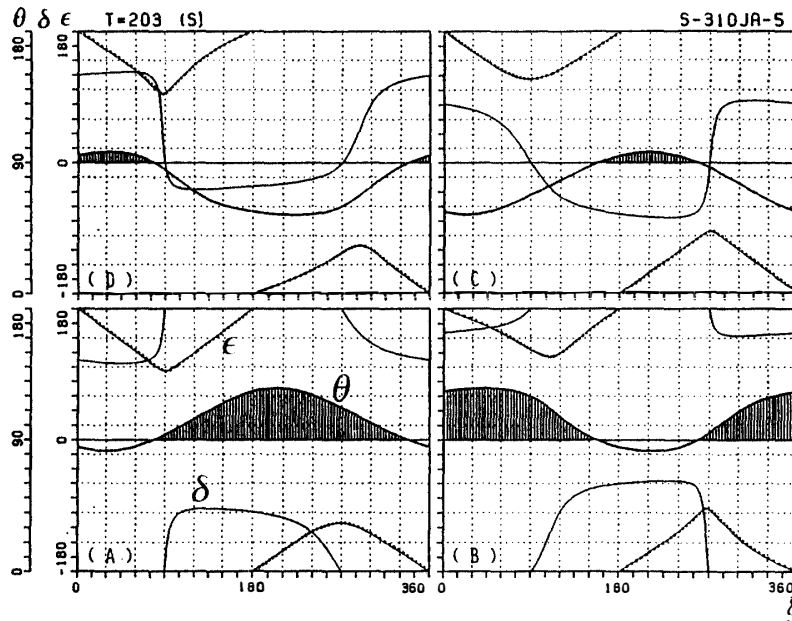
Fig. 9. ε, δ and θ versus ξ corresponding to cases (A) to (D) mentioned in the text. Hatched area for θ corresponds to θ>90°.

Actually for two cases, for solution i) $\varepsilon_1 = 135°$, $\delta_1 = -92°$ (case (A), $\xi = 135°$), and for solution ii) $\varepsilon_2 = -150°$, $\delta_2 = 145°$ (case (B), $\xi = 315°$).

For ray tracing, the electron density above an altitude of 200 km is assumed to be a diffusive equilibrium model with Te=800 K, and reference altitude=500 km, where $H^+ = 0.45\%$, $He^+ = 0.08\%$ and $O^+ = 99.47\%$. The electron density at 200 km is $1.8 \times 10^5/cc$, the value actually observed by the rocket. The electron density at the ISIS altitude (about 1400 km) is about $1.6 \times 10^2/cc$ for this model. The density profile used for the 3-D ray tracing is shown in Fig. 10, where the density profile of plasma temperature of 1000 K is also shown.

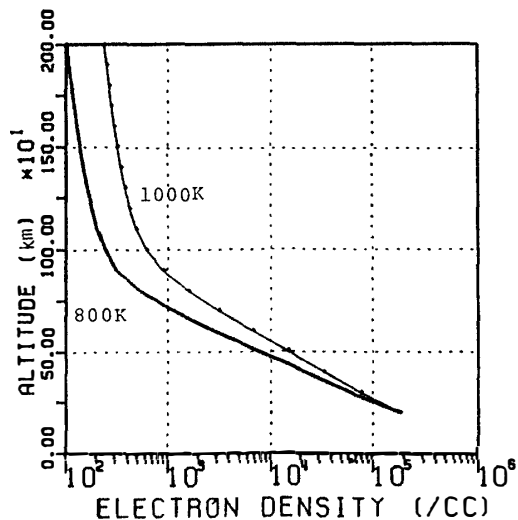According to the ray tracing for the wave normal directions observed at $t=203$ s

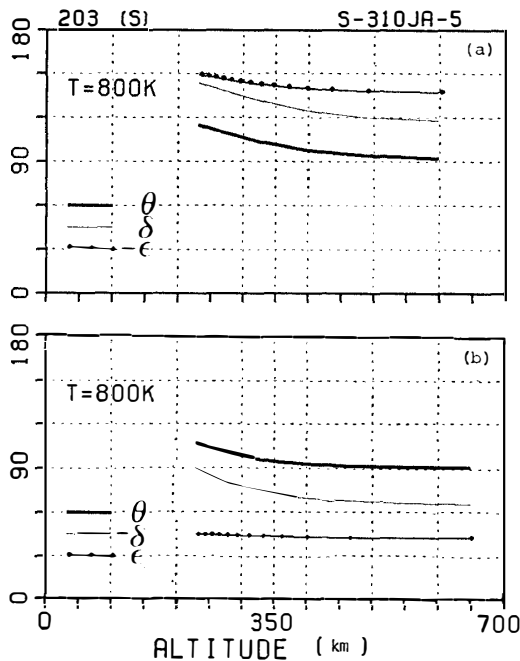Fig. 10. Electron density profiles above 200 km used for ray tracing.

Fig. 11. Results of ray tracing represented by θ, ε, and δ versus ξ for a temperature of 800 K and at 203 s after launch. (a) corresponds to the initial condition ii), and (b) corresponds to i). In case (b), the angle ε jumps from 135° to 45° at $-\delta=90°$ as $-\delta$ decreases from the initial value of 92°.

Table 1. Arrival wave normal directions.

Time	ξ	ε	δ
186 s	135°	137°	−106°
	300	−143	155
216 s	280	−119	161
	120	121	−106

and $h=221$ km, the angles ε, δ and θ along the backward ray path are as shown in Fig. 11, where the lower panel illustrates the ray path for the initial wave normal direction represented by ε_1, δ_1 and the upper panel by ε_2, δ_2. In both cases, the backward ray tracing stops at an altitude below 700 km. For two other sample times, $t=186$ and 216 s, the deduced incoming wave normal directions ξ, ε, and δ are listed in Table 1.

For all these initial wave normal directions, the backward ray paths always terminate at an altitude below 700 km. This fact implies that the source altitude of the observed hiss can not be higher than 700 km.

However, if the plasma temperature is increased up to 1000 K for example, *i.e.* the gradient of electron density profile becomes smaller, the ray path can be traced back to the opposite hemisphere like a nonducted whistler. Therefore, the gradient of the profile has an important role in ray path tracing. Actually, however, the electron density observed up to the apex of rocket, shown in Fig. 7, indicates that the gradient of the profile from 200 to 230 km to the apex of rocket is much steeper than that of the 800 K diffusive equilibrium model. Therefore, we can conclude that the source of the observed hiss can be at rather a low altitude, below 700 km.

4. Discussion and Conclusions

We have attempted to deduce the values of wave normal direction from the spin modulation pattern of the signal intensity of hiss, taking account of the direction of wave normal with reference to the rocket spin axis, observed by the rocket.

Spin modulation patterns are, however, not always stable enough, even if there are two sharp dips in signal intensity per spin period on the dynamic spectrum, so that the spin modulation pattern for every spin cycle is not always the same. It may be due to a time variation of the signal intensity or to a quick drift of the source location.

However, we can find relatively stable spin modulation patterns from which we can determine the incoming wave normal direction in a ground based rectangular coordinate system.

Generally, there are two possible directions, which may be interpreted as an ambiguity. However, for three different sample times after launch, $t=186$, 203 and 216 s, which correspond to the altitudes of 215, 221 and 224 km respectively, the derived directions of wave normal are roughly the same, 120° to 135° counter-clockwise from the geomagnetic north or 60° to 80° clockwise from GMN. This fact seems to be reasonable, although it is not enough evidence supporting our results.

In any case, the obtained wave normal directions were well away from the geomagnetic meridian plane making a large angle with geomagnetic field. As a result, the source of the auroral hiss observed must be located at rather low altitude, if the electron density decreases sharply for altitudes above the apex of the rocket. The plasma temperature we assumed is 800 K for the diffusive equilibrium model. But the gradient of the density profile based on this temperature is smaller than that observed for altitudes from 200 to 230 km, so that our conclusion may be reasonable.

References

KIMURA, I., MATSUO, T., TSURUDA, K. and YAMAGISHI, H. (1981): Measurements of the directions of propagation vector and Poynting flux of auroral hiss by means of the S-310JA-5 rocket. Mem. Natl Inst. Polar Res., Spec. Issue, 18, 439–452.
STIX, T. H. (1962): The Theory of Plasma Waves. New York, McGraw-Hill, 10.